Research Square

Preprints are preliminary reports that have not undergone peer review.
They should not be considered conclusive, used to inform clinical practice,
or referenced by the media as validated information.

Sequential development and evaluation of virtual model control with integral control for robotic dry-bone resection: a benchtop study

Ryan McWilliams
University of Cambridge
Daniel Larby
University of Cambridge
Fulvio Forni
University of Cambridge
Vikas Khanduja
vk279@cam.ac.uk

University of Cambridge

Research Article

Keywords: robotic surgery, orthopaedic robotics, bone resection, virtual model control, integral control, trajectory accuracy

Posted Date: September 11th, 2026

DOI: https://doi.org/10.21203/rs.3.rs-10856382/v1

License: This work is licensed under a Creative Commons Attribution 4.0 International License.
Read Full License

Additional Declarations: No competing interests reported.

Version of Record: A version of this preprint was published at Journal of Robotic Surgery on September 22nd, 2026. See the published version at https://doi.org/10.1007/s11701-026-03963-9.

Abstract

Purpose

Virtual model control (VMC) provides compliant trajectory execution, but sustained contact loads can produce residual positional error. This study evaluated the sequential development of VMC augmented with integral control for powered dry-bone resection and assessed the effects of end-effector stabilisation, spatial calibration and operating parameters.

Methods

A seven-degree-of-freedom Franka Research 3 robot was commanded using VMC with integral control and carried a 4-mm diamond-tipped arthroscopic burr through a programmed 10 x 10 mm serpentine trajectory in 20 pounds-per-cubic-foot synthetic bone. Four sequential configurations were assessed: an original handle-based mount, an anthropomorphically designed shaft-stabilising mount, robot-frame calibration and workpiece calibration. Each configuration comprised three resections. Performance was graded by one non-blinded assessor using a study-specific twelve-point score across burr-tip oscillation and X-, Y- and Z-axis deviation with lower scores indicating better performance. Radial depth of cut, engagement depth, trajectory velocity and burr angle were then screened to assess ideal operating parameters.

Results

Mean total score decreased sequentially from 11.7/12 with the original mount to 7.7/12 after shaft stabilisation, 5.7/12 after robot-frame calibration and 4.0/12 after workpiece calibration. The lowest observed score was maintained at an RDOC between 0.10 and 0.25 mm, a measured depth between 1.52 and 1.89 mm, velocity between 1.5 and 2.5 mm/s and a burr angle between 30 and 45 degrees.

Conclusion

Mechanical stabilisation and spatial calibration were associated with progressively better performances using VMC with integral control as a mechanism of robotic control. This exploratory benchtop study identified candidate ideal operating ranges for further assessment on higher-fidelity models.

Introduction

Cam-type femoroacetabular impingement (FAI) syndrome is a recognised cause of hip pain and impaired function in young and active adults [1]. It is associated with loss of sphericity at the femoral head–neck junction, which can produce abnormal contact with the acetabular rim and contribute to labral and chondral injury [2, 3]. Arthroscopic femoral osteochondroplasty aims to restore the physiological head–

neck contours and normalise joint contact stresses [4–6]. Randomised controlled trials have reported superior short-term patient-reported outcomes following arthroscopic surgery compared with structured non-operative treatment [7, 8], while registry data have demonstrated significant early improvement in patient-reported outcomes [9]. Achieving an accurate resection remains technically challenging [10]. Only part of the operative surface may be visible arthroscopically at any one time. Insufficient bone removal may leave residual cam morphology, which is a leading indication for revision hip arthroscopy [11]. Conversely, excessive resection can reduce femoral-neck strength and increase the risk of a fracture [12–14].

Robotic systems offer a means of translating a predefined surgical plan into a precisely controlled movement. Previous investigations have reported improved accuracy of cam correction using robotic or navigated techniques in synthetic-bone models and clinical cohorts [15–19]. Although, even when an appropriate trajectory has been defined, robotic resection performance remains dependent on the dynamic interaction between burr and bone.

The robotic platform examined in this study used virtual model control (VMC) with integral control. VMC represents the intended Cartesian motion as a virtual mechanism connected to the physical end effector through simulated stiffness and damping [20]. Differences in position and velocity between the virtual reference and the end effector generate corrective forces that are mapped to the robot joints. Although this compliant coupling facilitates surface interaction, a sustained contact force can deflect the end effector from its reference position. The integral control component accumulates this residual positional error and progressively increases the corrective response [21].

The present study evaluated the dynamic interaction between burr and bone whilst using VMC with integral control as a mechanism of robotic control. This was achieved through sequential stages of dry-bone resection whilst optimising various factors including mechanical stabilisation of the burr shaft, robot-frame calibration and workpiece registration in order to improve resection performance. The primary objective was to determine how these successive modifications affected burr oscillation and deviation from the programmed tool path. The secondary objective was to identify suitable ranges of radial depth of cut (RDOC), engagement depth, cutting velocity and burr angle for subsequent testing in an arthroscopic hip phantom.

Materials and methods

Study design

A staged benchtop development and evaluation study comprising five sequential experiments was performed. Experiment I established dry-bone resection using the original burr mount. Experiment II introduced a custom anthropomorphically designed shaft-stabilising mount. Experiment III added calibration between the software representation and the physical robot. Experiment IV added registration

of the operating surface. Experiment V varied four operating parameters to identify the ideal performance ranges.

Robotic platform and cutting system

A seven-degree-of-freedom Franka Research 3 robotic arm (Franka Emika, Munich, Germany) was used. The robot carried a Stryker CrossBlade XL Diamond Burr (Stryker, Kalamazoo, USA). The 4-mm diamond burr was operated at 12,000 revolutions per minute. A synthetic bone block with a density of 20 pounds per cubic foot (PCF) was fixed within a benchtop vice. The complete benchtop arrangement is shown in Fig. 1a.

The original mount primarily constrained the burr handle. Because the burr incorporated a removable shaft, compliance was observed at the shaft-handle interface. A revised mount was designed using three-dimensional computer-aided design and manufactured by three-dimensional printing. Inspired by the grip used by hip-preservation surgeons, the mount enclosed and supported the proximal shaft while retaining sufficient exposed distal shaft for future arthroscopic access. Two rubber O-rings restricted rotation within the mount and reduced transmission of vibration. The original and revised mounting arrangements are shown in Fig. 1.

Virtual model control with integral control and programmed trajectory

The motion trajectory and VMC with integral control were implemented in the Julia programming language using Visual Studio Code (Microsoft, Washington, USA). The desired trajectory was represented by a virtual Cartesian 'cart', and the physical end effector was coupled to this reference through virtual stiffness and damping.

The end effector moved from an idle pose to a predefined task-start pose while achieving the required orientation at a velocity proportional to the distance from the start pose. It then approached the bone along the Z-axis at 2.5 mm/s. The burr was activated manually before contact. A serpentine raster trajectory was executed in which the burr traversed the 10-mm square along the X-axis, advanced in the negative Y-direction by the programmed RDOC, returned along the X-axis and repeated the cycle until the square was covered. It then withdrew along the Z-axis before the burr was deactivated. The burr was maintained at 45 degrees to the bone surface in Experiments I-IV.

Sequential mechanical modification and spatial calibration

Experiment I used the original mount to resect three 10 x 10 mm squares. Experiment II repeated the task with the custom shaft-stabilising mount. In Experiment III, infrared reflective markers were attached to the robot links and end effector. An OptiTrack motion-capture system (NaturalPoint Inc., Corvallis,

USA) measured the position and orientation of the marker configurations, enabling alignment of the robot-base and end-effector coordinate frames and the virtual model. Experiment IV registered the workpiece by placing the burr tip at four distinct points on three surfaces of the synthetic block. The combined point measurements defined the position and orientation of the operating zone, allowing the programmed square to be aligned with the physical bone surface and compensating for imprecision in manual placement within the benchtop vice.

Operating-parameter characterisation

Following mechanical stabilisation and spatial calibration, experiment V, assessed four parameters individually while the remaining parameters were maintained at the standard configuration: RDOC, programmed engagement depth, trajectory velocity and the angle between the burr shaft and bone surface. RDOC values of 0.10, 0.15, 0.20, 0.25, 0.30 and 0.40 mm were tested. Attempted resection depths were 0.50, 1.00, 1.50, 2.00, 2.50 and 3.00 mm with actual measured depths being 0.64, 0.86, 1.52, 1.89, 2.67 and 3.06 mm respectively. Depth was measured using a depth gauge. Velocities of 1.5, 2.0, 2.5, 3.0 and 3.5 mm/s and burr angles of 15, 30, 45, 60 and 75 degrees were assessed.

Outcome assessment

Tool-path deviation was defined as the linear difference between the programmed and observed burr-tip position arising during robot-bone interaction. Oscillation was defined as visible vibration of the burr tip during contact. Slow-motion footage was reviewed frame by frame by one assessor who was non-blinded. Rulers in the X- and Y-axes provided a scale, and the camera was positioned above the operating zone to reduce perspective distortion. Z-axis deviation was assessed using measured resection depth. Surface material and video footage were reviewed for endpoint deviation, and the difference between physical and programmed endpoints was recorded when deviation occurred in the direction of travel.

Four domains were graded: visible oscillation, X-axis deviation, Y-axis deviation and Z-axis deviation. Each received 0 points for no measurable oscillation/deviation, 1 point for approximately 1 mm, 2 points for approximately 2 mm and 3 points for 3 mm or greater. Domain scores were summed to produce a total from 0 to 12, with lower scores indicating closer adherence to the planned trajectory. Because the high-frequency burr-tip movement exceeded the temporal resolution needed for plane-specific vibration analysis, oscillation was graded as a single overall domain rather than separately in each axis.

Analysis

Results were summarised descriptively. For Experiments I-IV, individual total scores and means are reported. Formal hypothesis tests and confidence intervals were not used because each sequential configuration comprised three resections, the composite outcome was ordinal and the study was not

designed or powered for inferential comparisons. Experiment V observations were used to define candidate settings for subsequent replicated testing.

Results

Initial powered resection

All three squares in Experiment I demonstrated visible oscillation and deviations in each spatial axis. X- and Y-axis deviations were at least 3 mm in every attempt; Z-axis deviation was at least 3 mm in two attempts and 2 mm in one. Total scores were 12, 11 and 12 (mean 11.7).

Effect of shaft stabilisation and calibration

In Experiment II, the shaft-stabilising mount reduced visible burr-tip oscillation to approximately 1 mm in all three resections. X- and Y-axis deviations were 2 mm and Z-axis deviation remained between 2 and 3 mm. Total scores were 8, 7 and 8 (mean 7.7). The resection surface changed from a cratered topography to a smoother, wave-like finish, although the intended square retained a rhomboid appearance (Fig. 2a, b).

In Experiment III, robot-frame calibration produced further improvement. Mean X- and Y-axis scores of 1.3 and a mean Z-axis score of 2.0. Total scores were 6, 5 and 6 (mean 5.7) Surface topography became smoother, although one side remained deeper and produced a scalloped base. After workpiece calibration in Experiment IV, every resection scored 1 in all four domains, giving a mean score of 4. The resulting squares had a visually level base, more linear margins and corners that more closely approximated right angles. These sequential changes in surface appearance are shown in Fig. 2. The mean total score decreased by 7.7 points between Experiments I and IV (Table 1 and Fig. 3).

Table 1
Domain and total performance scores across sequential development.

Experiment	Configuration	Oscillation	X	Y	Z	Total score
I	Original mount	3.0	3.0	3.0	2.7	11.7 (12, 11, 12)
II	Stabilising mount	1.0	2.0	2.0	2.7	7.7 (8, 7, 8)
III	Robot calibration	1.0	1.3	1.3	2.0	5.7 (6, 5, 6)
IV	Workpiece calibration	1.0	1.0	1.0	1.0	4.0 (4, 4, 4)

Key: Domain and total values are means; individual total scores are shown in parentheses. Lower scores indicate better performance.

Operating-parameter characterisation

In Experiment V, the lowest observed total score of 4 was achieved across RDOC values of 0.10–0.25 mm. Scores increased to 5 at 0.30 mm and 6 at 0.40 mm, driven mainly by Y- and Z-axis deviations. Although RDOC values as low as 0.10 mm maintained the same observed score, 0.20–0.25 mm provided the preferred efficiency-performance balance.

For depth, the best score of 4 occurred at measured depths of 1.52 and 1.89 mm. Shallower measured depths of 0.64 and 0.86 mm scored 5 because oscillation increased to 2 mm. Deeper cuts of 2.67 and 3.06 mm scored 6, with increased Y- and Z-axis deviation. The mean absolute error between attempted and measured depth was 0.11 mm.

Velocities of 1.5, 2.0 and 2.5 mm/s each scored 4. Performance deteriorated at 3.0 mm/s (score 6) and 3.5 mm/s (score 7), with increased oscillation and spatial deviation. Burr angles of 30 and 45 degrees scored 4; performance was lower at 15 degrees (score 5), 60 degrees (score 6) and 75 degrees (score 7). The recorded data therefore supported the expected ideal operating parameters of RDOC 0.10–0.25 mm, measured depth 1.52–1.89 mm, velocity 1.5–2.5 mm/s and angle 30–45 degrees. Efficiency considerations favoured RDOC 0.20–0.25 mm and velocity 2.0-2.5 mm/s (Fig. 4).

Discussion

This study describes the sequential development and exploratory evaluation of VMC with integral control for dry-bone resection. First, the original handle-based mount did not adequately constrain the burr shaft during bone contact; supporting the proximal shaft was associated with less visible oscillation and a lower performance score. Second, calibration of the physical robot and then the workpiece produced further incremental changes, particularly in Z-axis depth uniformity. Third, the parameter screen identified candidate ranges in which the lowest observed score was maintained: RDOC 0.10–0.25 mm, measured depth 1.52–1.89 mm, velocity 1.5–2.5 mm/s and angle 30–45 degrees. Across the sequential configurations, the mean score decreased from 11.7 to 4.0.

Contact between the diamond tipped burr and synthetic bone produced rapid, irregular displacement of the burr tip. We used the descriptive term 'stochastic jumping' for this behaviour, hypothesising that contact depended on the distribution of bone particles, the orientation at which individual diamond particles contacted the bone, and the position and orientation of each particle within the resection zone. When the shaft-handle interface remained compliant, motion was not transmitted rigidly to the burr tip. The tip lagged behind the mount, particularly at direction changes, contributing to acute cornering, widened channels and residual bone islands.

The shaft-stabilising mount was deliberately surgeon-inspired. Experienced surgeons were observed to stabilise the burr closer to the shaft rather than relying solely on the handle, shortening the unsupported shaft. The revised mount reproduced this principle and incorporated O-rings to resist rotation and damp vibration. Adding mechanical support improved the average performance score by four points and produced a smoother resection surface.

Robot-frame calibration aligned the software representation with the physical base and end-effector frames. X- and Y-axis scores were lower after this stage, but the resection remained deeper on one side because manual workpiece levelling was not sufficiently aligned to the robot's physical base and end-effector frames. Registration of three workpiece planes then allowed the trajectory to be expressed relative to the operating zone, and the mean Z-axis score decreased from 2.0 to 1.0. This distinction between robot calibration and workpiece registration is consistent with literature, in which alignment among image, tracker, instrument and patient coordinate frames is central to executing a planned resection [19, 22].

Increasing RDOC increased the resected volume during each pass and was associated with greater lateral and depth deviation above 0.25 mm. Engagement beyond approximately half the 4-mm burr diameter created an overhanging bone edge that could be struck during oscillation, which may explain the higher scores at measured depths above 2 mm. Conversely, very shallow cuts showed more oscillation and would require additional passes. Velocity above 2.5 mm/s may have reduced the time available for the compliant system to establish stable contact with the bone and was associated with worse performance scores. Angles between 30 and 45 degrees provided the lowest scores within the tested range; steeper angles increased lateral and depth deviation, while the shallowest angle increased X-axis deviation.

This work identified two requirements for the next system iteration. First, calibration accuracy declined during repeated testing and required periodic manual recalibration. An optical tracking system should therefore remain active during resection and continuously update the position error between the burr tip and workpiece. Secondly, this optical tracking system should also provide a more objective outcome measure and allow tracking error to be analysed over time and by axis, as millimetre-level slow-motion footage grading is insufficient for detailed controller optimisation.

This study has several limitations. Each sequential configuration was assessed using only three resections and assessment was performed by a single non-blinded assessor. Formal statistical inference was therefore not appropriate, and the observed changes should be interpreted as descriptive findings rather than proof of superiority. Finally, the homogeneous 20-PCF block did not reproduce anatomy, cortical-cancellous transitions, soft tissue or an arthroscopic portal.

Conclusion

Sequential mechanical stabilisation and spatial calibration enabled a robotic arm commanded by VMC with integral control to progress from unstable cuts to repeatable resections in a synthetic-bone block. In this descriptive evaluation, the mean performance score decreased from 11.7/12 to 4.0/12. after optimisations. Optimal performance was maintained within parameter ranges of RDOC 0.10–0.25 mm, measured depth 1.52–1.89 mm, velocity 1.5–2.5 mm/s and burr angle 30–45 degrees. Continuous optical tracking should monitor the relative positions of the burr and bone throughout resection. Higher-

fidelity testing is recommended under simulated arthroscopic conditions such as a hip phantom containing dry-bone models with FAI morphology before clinical readiness can be evaluated.

Declarations

Competing interests:

No competing interests to declare.

Ethics approval:

Not applicable. This bench study involved no human participants, human data, animals or biological material.

Funding:

This work was supported by grant funding received from The Observatory for Human-Machine Collaboration, University of Cambridge.

Author Contribution

RM: conceptualisation; methodology; software; investigation; analysis; writing; editing. DL: software; investigation; editing. FF: conceptualisation; methodology; software; editing; funding acquisition; project oversight. VK: conceptualisation; methodology; editing; funding acquisition; project oversight.

Acknowledgement

Large language model, OpenAI’s GPT 5.6, was used to improve language and formatting during the editing process. It was not used to generate, alter or analyse experimental data.

Data and code availability:

Slow-motion video footage and the Julia controller code alongside controller parameter metrics are available from the corresponding author on reasonable request.

References

1. Imam S, Khanduja V (2011) Current concepts in the diagnosis and management of femoroacetabular impingement. Int Orthop 35:1427–1435. https://doi.org/10.1007/s00264-011-1278-7
2. Ganz R, Parvizi J, Beck M, Leunig M, Nötzli H, Siebenrock KA (2003) Femoroacetabular impingement: a cause for osteoarthritis of the hip. Clin Orthop Relat Res 417:112–120. https://doi.org/10.1097/01.blo.0000096804.78689.c2
3. Yarwood W, Sunil Kumar KH, Ng KCG, Khanduja V (2022) Biomechanics of cam femoroacetabular impingement: a systematic review. Arthroscopy 38:174–189. https://doi.org/10.1016/j.arthro.2021.05.066
4. Khanduja V, Villar RN (2007) The arthroscopic management of femoroacetabular impingement. Knee Surg Sports Traumatol Arthrosc 15:1035–1040. https://doi.org/10.1007/s00167-007-0319-7
5. Khanduja V, Ha YC, Koo KH (2021) Controversial issues in arthroscopic surgery for femoroacetabular impingement. Clin Orthop Surg 13:437–442. https://doi.org/10.4055/cios21109
6. Van Houcke J, Khanduja V, Audenaert EA (2021) Accurate arthroscopic cam resection normalizes contact stresses in patients with femoroacetabular impingement. Am J Sports Med 49:42–48. https://doi.org/10.1177/0363546520974378
7. Griffin DR, Dickenson EJ, Wall PDH et al (2018) Hip arthroscopy versus best conservative care for the treatment of femoroacetabular impingement syndrome (UK FASHIoN): a multicentre randomised controlled trial. Lancet 391:2225–2235. https://doi.org/10.1016/S0140-6736(18)31202-9
8. Palmer AJR, Ayyar Gupta V, Fernquest S et al (2019) Arthroscopic hip surgery compared with physiotherapy and activity modification for the treatment of symptomatic femoroacetabular impingement: multicentre randomised controlled trial. BMJ 364:l185. https://doi.org/10.1136/bmj.l185
9. Holleyman R, Sohatee MA, Lyman S, Malviya A, Khanduja V, NAHR User Group (2023) Hip arthroscopy for femoroacetabular impingement is associated with significant improvement in early patient reported outcomes: analysis of 4963 cases from the UK non-arthroplasty registry (NAHR) dataset. Knee Surg Sports Traumatol Arthrosc 31:58–69. https://doi.org/10.1007/s00167-022-07042-y
10. Nakano N, Audenaert E, Ranawat A, Khanduja V (2018) Review: current concepts in computer-assisted hip arthroscopy. Int J Med Robot 14:e1929. https://doi.org/10.1002/rcs.1929
11. Ross JR, Larson CM, Adeoye O, Kelly BT, Bedi A (2015) Residual deformity is the most common reason for revision hip arthroscopy: a three-dimensional CT study. Clin Orthop Relat Res 473:1388–1395. https://doi.org/10.1007/s11999-014-4069-9
12. Mardones RM, Gonzalez C, Chen Q, Zobitz M, Kaufman KR, Trousdale RT (2005) Surgical treatment of femoroacetabular impingement: evaluation of the effect of the size of the resection. J Bone Joint Surg Am 87:273–279. https://doi.org/10.2106/JBJS.D.01793

13. Wijdicks CA, Balldin BC, Jansson KS, Stull JD, LaPrade RF, Philippon MJ (2013) Cam lesion femoral osteoplasty: in vitro biomechanical evaluation of iatrogenic femoral cortical notching and risk of neck fracture. Arthroscopy 29:1608–1614. https://doi.org/10.1016/j.arthro.2013.06.021
14. Horner NS, Khanduja V, MacDonald AE, Naendrup JH, Simunovic N, Ayeni OR (2017) Femoral neck fractures as a complication of hip arthroscopy: a systematic review. J Hip Preserv Surg 4:9–17. https://doi.org/10.1093/jhps/hnw048
15. Masjedi M, Tan WL, Jaskaranjit S, Aqil A, Harris S, Cobb J (2013) Use of robotic technology in cam femoroacetabular impingement corrective surgery. Int J Med Robot 9:23–28. https://doi.org/10.1002/rcs.1486
16. Park CN, Nawabi DH, Christopher J, Conditt MA, Ranawat AS (2015) Robotic-assisted femoral osteochondroplasty is more precise than a freehand technique in a Sawbone model. J Hip Preserv Surg 2:136–144. https://doi.org/10.1093/jhps/hnv007
17. Almoussa S, Barton C, Speirs AD, Gofton W, Beaulé PE (2011) Computer-assisted correction of cam-type femoroacetabular impingement: a Sawbones study. J Bone Joint Surg Am 93 Suppl 270–75. https://doi.org/10.2106/JBJS.J.01706
18. Van Houcke J, Khanduja V, Nakano N, Krekel P, Pattyn C, Audenaert E (2017) Accuracy of navigated cam resection in femoroacetabular impingement: a randomised controlled trial. Int J Med Robot 13:e1839. https://doi.org/10.1002/rcs.1839
19. Abe K, Oba M, Kobayashi N, Higashihira S, Choe H, Tezuka T, Ike H, Inaba Y (2022) Accuracy of computer navigation-assisted arthroscopic osteochondroplasty for cam-type femoroacetabular impingement using the model-to-image registration method. Am J Sports Med 50:1272–1280. https://doi.org/10.1177/03635465221074338
20. Larby D, Forni F (2023) A generalized approach to impedance control design for robotic minimally invasive surgery. IFAC-PapersOnLine 56:8548–8555. https://doi.org/10.1016/j.ifacol.2023.10.015
21. Larby D, Forni F (2026) Optimal virtual model control for robotics: design and tuning of passivity-based controllers. IEEE Trans Robot 42:439–454. https://doi.org/10.1109/TRO.2025.3645886
22. Audenaert EA, Smet B, Pattyn C, Khanduja V (2012) Imageless versus image-based registration in navigated arthroscopy of the hip: a cadaver-based assessment. J Bone Joint Surg Br 94:624–629. https://doi.org/10.1302/0301-620X.94B5.28627

Figures

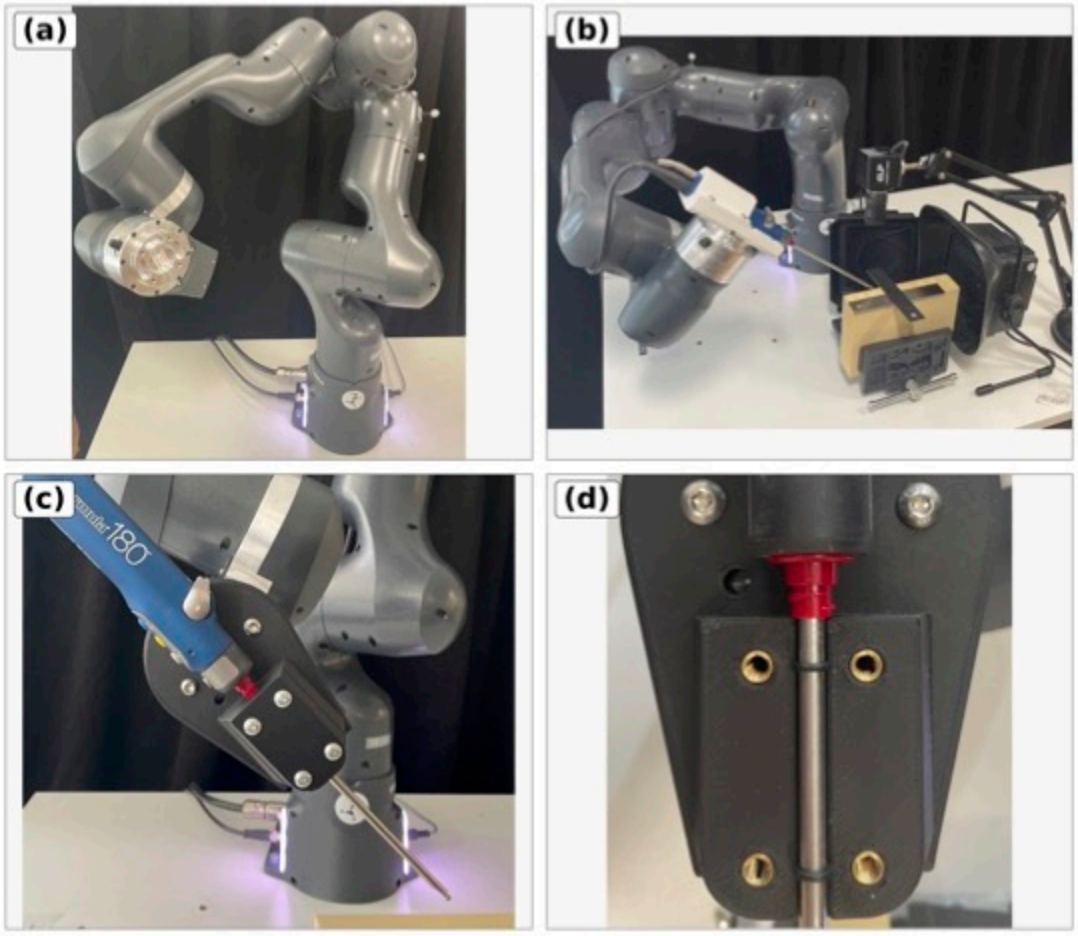


Figure 1

Experimental platform and development of the burr-mounting system. (a) Franka Research 3 robot used for benchtop testing. (b) Original handle-based burr-mounting configuration with a fixed synthetic-bone block. (c) Revised custom mount supporting the proximal burr shaft while leaving the distal shaft exposed for bone engagement. (d) Close-up of the mount interior, showing the proximal shaft support and the two O-rings surrounding the burr shaft.

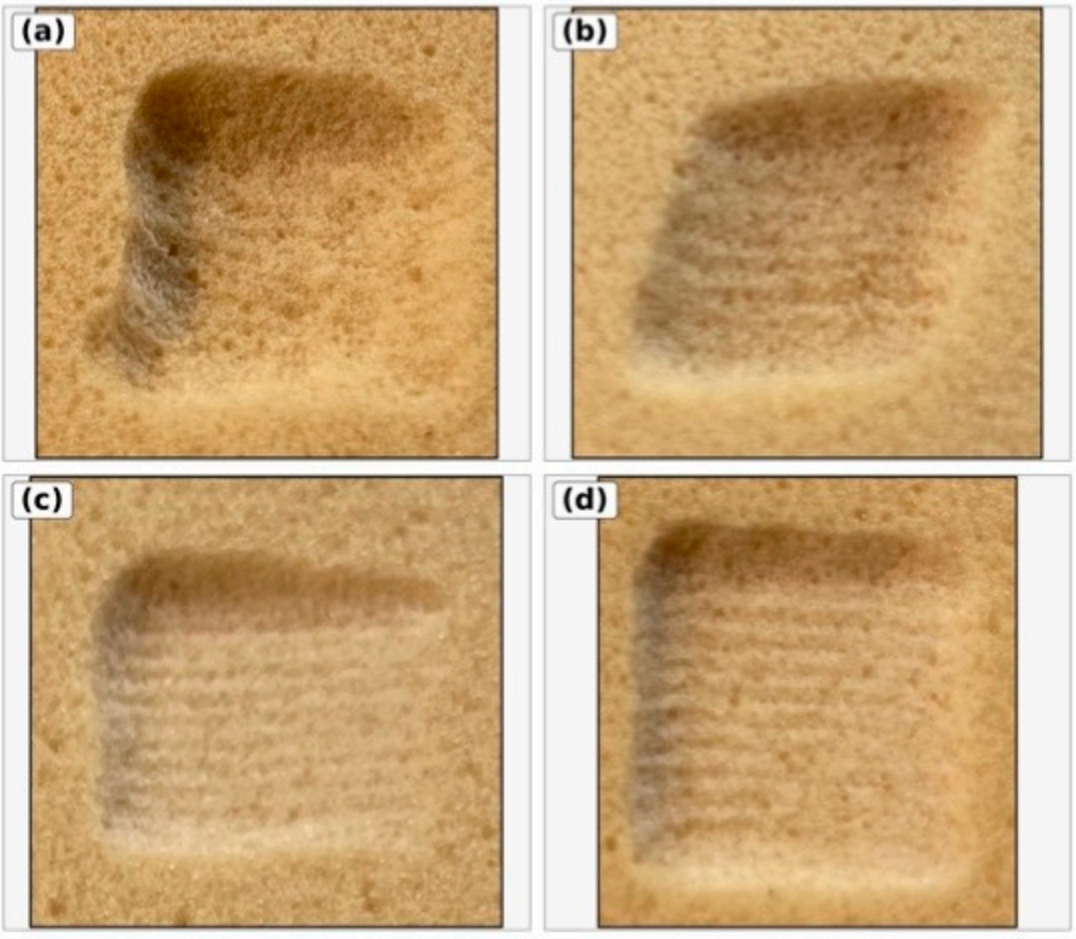


Figure 2

Progressive changes in dry-bone resection during sequential system development. Panels (a)-(d) show representative resections from Experiments I-IV, respectively. The sequence illustrates the transition from an irregular, localised resection to a broader, more clearly defined square.

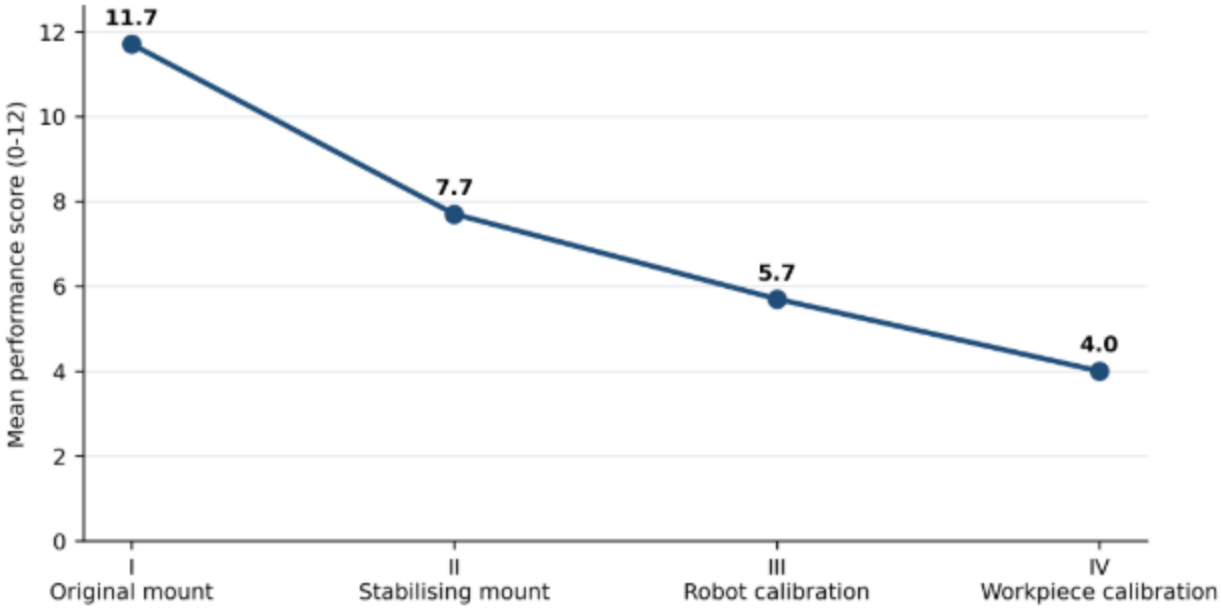


Figure 3

Sequential improvement in mean performance score. Each configuration comprised three 10 x 10 mm resections. Lower scores indicate less oscillation and trajectory deviation.

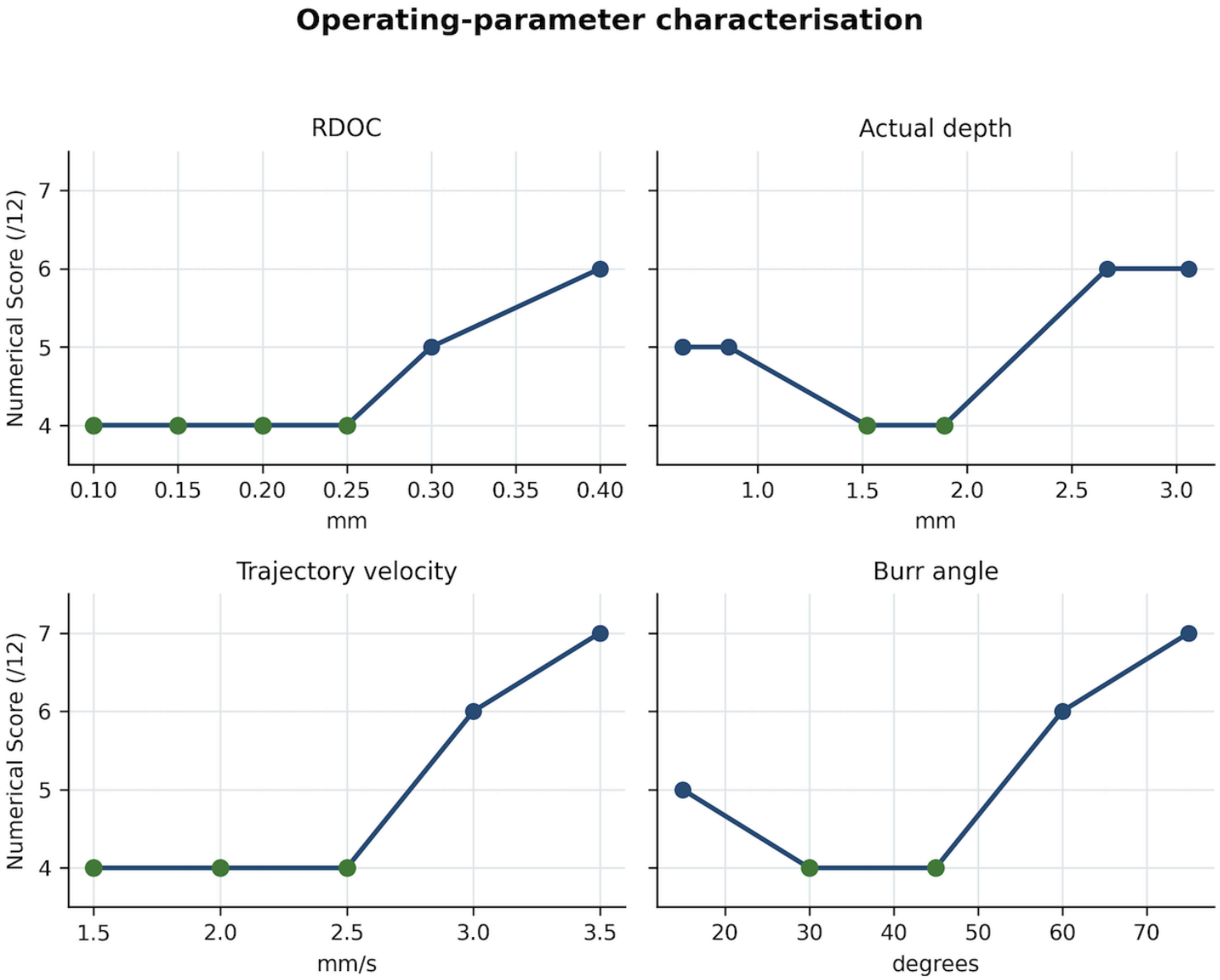


Figure 4

Performance score across RDOC, measured engagement depth, trajectory velocity and burr angle. Green markers indicate settings attaining the best observed score of 4. Each parameter was varied individually. The composite score was a numerical scoring system out of 12 with lower scores indicating a closer adherence to the planned trajectory.